arXiv:1611.01981v1 [cond-mat.str-el] 7 Nov 2016

Optical Process of Linear Dichroism in Angle-Resolved Core-Level Photoemission Reflecting the Strongly Correlated Anisotropic Orbital Symmetry

Akira Sekiyama,[1,2] Yuina Kanai,[1,2] Arata Tanaka,[3] and Shin Imada[2,4]

[1]*Division of Materials Physics, Graduate School of Engineering Science, Osaka University, Toyonaka, Osaka 560-8531, Japan*
[2]*RIKEN SPring-8 Center, Sayo, Hyogo 679-5148, Japan*
[3]*Department of Quantum Matter, ADSM, Hiroshima University, Higashi-Hiroshima, Hiroshima 739-8530, Japan*
[4]*Department of Physical Science, Ritsumeikan University, Kusatsu, Shiga 525-8577, Japan*

(Dated: November 8, 2016)

We revisit the formulations and simulations of angular distributions in polarization-dependent core-level photoemission spectra of strongly correlated electron systems for the explanation of recently discovered linear dichroism in the core-level photoemission of $4f$-based rare-earth compounds. Owing to the selection rules for the optical process of core-level excitations, the linear dichroism (LD) originating from the anisotropic outer localized charge distributions determined by the ground-state orbital symmetry can be observed. Our simulations show that the d-orbital core-level excitations are essential for the LD for localized ions in cubic symmetry, which is absent in the p-orbital excitations.

Ground- and excited-states orbital symmetry or orbital polarization in strongly correlated electron systems has crucial roles in their functional properties. For example, highly two-dimensional characters of the conducting carriers in high-temperature superconducting cuprates are due to their Cu $3d_{x^2-y^2}$ orbital symmetry split by the effective crystalline electric field (CEF) mixed with the O $2p_{x,y}$ symmetry in the CuO_2 planes[1–3]. Strongly correlated $4f$-based heavy Fermion compounds show a variety of intriguing phenomena such as unconventional superconductivity[4–7], multipole ordering[8–10], and both successive transitions[11] as a function of temperature. The CEF-split ground-state $4f$-orbital symmetry of such compounds is very fundamental for examining their properties.

However, the $4f$-orbital symmetry had not been straightforwardly revealed for realistic materials, as seen in an old controversy for CeB_6 (Ref. 12). There are too many adjustable parameters to uniquely determine the symmetry by an analysis of inelastic neutron scattering and anisotropy in magnetic susceptibility, which has been recognized as an standard experimental technique. Inelastic polarized neutron scattering[13] is useful but time-consuming and requires a large single-crystalline sample. On the other hand, such x-ray spectroscopic techniques as linear dichroism (LD) in soft-X-ray absorption (XAS) near rare-earth $M_{4,5}$ edges[13–18] and polarization-dependent non-resonant inelastic x-ray scattering[19] (NIXS) have been much improved for probing the anisotropic $4f$ charge distributions derived from the orbital symmetry.

Recently, it has been reported that the ground-state $4f$-orbital symmetry can be uniquely determined by linear polarization-dependent angle-resolved core-level photoemission of Yb compounds not only in tetragonal symmetry[20] but also in cubic symmetry[21]. This technique will be promising for revealing the ground- and excited-state orbital symmetry of strongly correlated electron systems, being complementary to LD-XAS and LD-NIXS. There is an advantage in the applicability to the systems in cubic symmetry for the LD in angle-resolved core-level photoemission of the system with localized anisotropic outer charge distributions.

In this paper, we show the formulations and simulations of the polarization-dependent angle-resolved core-level photoemission including so called transition matrix elements, which describe the transition probabilities between the initial and final states. One can recognize that LD in the spectra is intrinsically observed for partially filled $4f$ systems even in cubic symmetry by the formulations. These have been a long-standing pitfall in photoemission spectroscopy of solids. The matrix elements in angle-resolved valence-band photoemission have been previously discussed[22–25]. The photoionization cross-sections and asymmetry parameters for core-level photoemission of ions with spherical charge distributions have already been established[26–30]. Nevertheless, the combined formulations of the core-level photoemission for the strongly correlated systems with the emission angle- and polarization-dependent matrix elements have been lacking to date.

In the core-level photoemission process, one inner-core electron with the quantum numbers $\lambda_c \equiv (n_c l_c m_c s_c)$ is removed from the strongly correlated sites in the final states, where n_c, l_c, m_c, and s_c denotes the principal, orbital, magnetic, and spin quantum numbers. The $n_c l_c$ core-level photoemission spectra of the strongly correlated electron systems have so far been expressed using an angle-integrated form[31,32] as a function of energy $\omega \equiv E_K^* - h\nu$ of

$$\rho(\omega) = \sum_{n,m_c,s_c} |\langle E_f^{(n)}(\underline{\lambda_c})|a_{\lambda_c}|E_i\rangle|^2 \delta(\omega + E_f^{(n)}(\underline{\lambda_c}) - E_i), \tag{1}$$

where E_i and $E_f^{(n)}(\underline{\lambda_c})$ stand for the initial-state energy and the eignenergy of one of the final states (n) with the core hole $\underline{\lambda_c}$, and E_K^* denotes the photoelectron kinetic energy in a solid. For the ions with the atomic-like

partially filled subshell, the one-electron-removal state $a_{\lambda_c}|E_i\rangle$ is generally no longer the eigenstate of $|E_f^{(n)}(\underline{\lambda_c})\rangle$ due to the anisotropy in Coulomb and exchange interactions between the outer electron and created core hole, which leads to the multiplet-split multiple-peak structure in the core-level spectra. For obtaining Eq. 1, it is assumed that the matrix elements M_{λ_c} have negligible emission angle and polarization dependence within the $n_c l_c$ core-level excitations. In order to understand LD in the angle-resolved core-level photoemission spectra of a single crystal, however, we need to start from the form in which M_{λ_c} is explicitly taken into account as

$$\rho(\omega,\vec{e},\theta_k,\varphi_k)=\sum_{n,m_c,s_c}|M_{\lambda_c}\langle E_f^{(n)}(\underline{\lambda_c})|a_{\lambda_c}|E_i\rangle|^2\delta(\omega+E_f^{(n)}(\underline{\lambda_c})-E_i), \tag{2}$$

where $\vec{e}$ is the unit vector indicating the electric field direction of the excitation light, and θ_k and φ_k denote the polar and azimuthal angles of observed photoelectrons.

For simplicity, let us discuss the core-level photoemission process from the single ion under CEF within the electric dipole transitions. The photoelectron wavefunction excited from the inner core state λ_c with the atomic-like one-electron wavefunction

$$R_{n_c l_c}(r)Y_{l_c}^{m_c}(\theta,\varphi) \tag{3}$$

can be represented as

$$4\pi\sum_{l',m'}(\mathrm{i})^{l'}e^{-\mathrm{i}\delta_{l'}}Y_{l'}^{m'*}(\theta_k,\varphi_k)R_{kl'}(r)Y_{l'}^{m'}(\theta,\varphi) \tag{4}$$

by means of the partial wave expansion[22–25], where $\delta_{l'}$ stands for the phase shift and the radial function $R_{kl'}(r)$ is for the continuum state with the photoelectron momentum $k=|\vec{k}|=\sqrt{2mE_K^*}/\hbar$. Equation 4 shows the asymptotic behavior at $|\vec{r}|\to\infty$ as $\sim\exp(\mathrm{i}\vec{k}\cdot\vec{r})/r$. Due to the selection rules for the dipole transitions, l' is restricted as $l'=l_c\pm1$ whereas $m'=m_c$ $(m_c\pm1)$ for $\vec{e}\parallel z=r\cos\theta$ $(\vec{e}\perp z)$. Then we obtain the transition matrix elements M_{λ_c} from Eqs. 3 and 4 as

$$M_{\lambda_c}=4\pi\sum_{l',m'}(\mathrm{i})^{-l'}e^{\mathrm{i}\delta_{l'}}Y_{l'}^{m'}(\theta_k,\varphi_k)\iiint R_{kl'}^*(r)Y_{l'}^{m'*}(\theta,\varphi)(\vec{e}\cdot\vec{p})R_{n_c l_c}(r)Y_{l_c}^{m_c}(\theta,\varphi)dV, \tag{5}$$

where $dV=r^2\sin\theta dr d\theta d\varphi$ and $\vec{p}$ is the momentum operator $-\mathrm{i}\hbar\nabla$. If the interference effects between outgoing l_c+1 and l_c-1 photoelectron waves are negligible, the polarization-dependent angle-resolved $n_c l_c$ core-level photoemission spectra can be represented from Eqs. 2 and 5 as

$$\rho(\omega,\vec{e},\theta_k,\varphi_k)=\sum_{n,m_c,s_c}\sum_{l'}\left|\sum_{m'}Y_{l'}^{m'}(\theta_k,\varphi_k)A_{\lambda_c}^{kl'm'}(\vec{e})\langle E_f^{(n)}(\underline{\lambda_c})|a_{\lambda_c}|E_i\rangle\right|^2\delta(\omega+E_f^{(n)}(\underline{\lambda_c})-E_i), \tag{6}$$

where

$$A_{\lambda_c}^{kl'm'}(\vec{e})=4\pi\iiint R_{kl'}^*(r)Y_{l'}^{m'*}(\theta,\varphi)(\vec{e}\cdot\vec{p})R_{n_c l_c}(r)Y_{l_c}^{m_c}(\theta,\varphi)dV. \tag{7}$$

Furthermore, when the $l_c\to l_c+1$ transitions are much predominant over the $l_c\to l_c-1$ transitions[23,33], under the approximation of which the experimental polarization-dependent angle-resolved Yb^{3+} $3d_{5/2}$ core-level photoemission spectra have been well reproduced by the spectral simulations[20,21], we obtain

$$\rho(\omega,\vec{e},\theta_k,\varphi_k)\simeq\sum_{n,m_c,s_c}\left|\sum_{m'}Y_{l_c+1}^{m'}(\theta_k,\varphi_k)A_{\lambda_c}^{k(l_c+1)m'}(\vec{e})\langle E_f^{(n)}(\underline{\lambda_c})|a_{\lambda_c}|E_i\rangle\right|^2\delta(\omega+E_f^{(n)}(\underline{\lambda_c})-E_i). \tag{8}$$

Comparing Eq. 8 with Eq. 1, one can recognize that the spectral weights of the multiplet-split peaks are modulated from those in the isotropic spectral function by the terms of $Y_{l_c+1}^{m'}(\theta_k,\varphi_k)$ and $A_{\lambda_c}^{k(l_c+1)m'}(\vec{e})$ in the

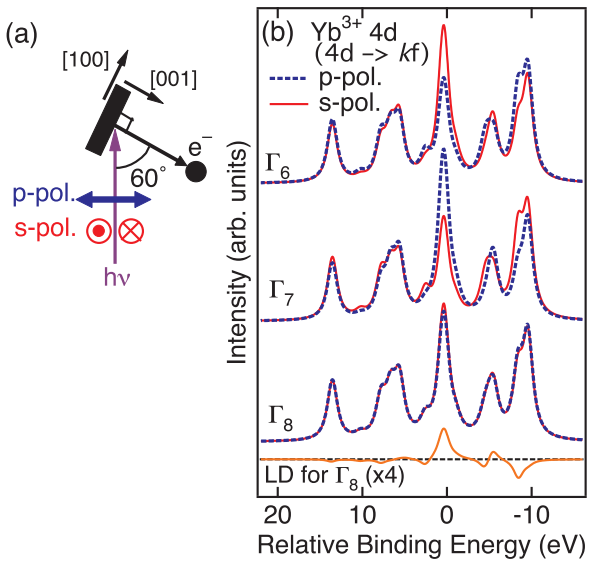

FIG. 1. (Color online) (a) Geometry for polarization-dependent angle-resolved core-level photoemission. (b) Simulated polarization-dependent $4d$ core-level photoemission spectra along the [001] direction of Yb^{3+} ions assuming the CEF-split ground state in cubic symmetry. The relative binding energy corresponds to $-\omega$. Gaussian and Lorentzian broadenings have been set to 0.4 and 1.2 eV, respectively, as full widths at half maximum (FWHM). The spectra have been normalized by the overall $4d$ spectral weight. LD for the Γ_8 ground state is also shown.

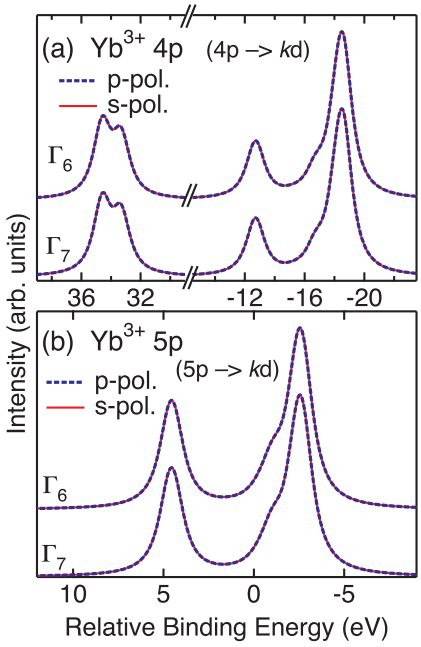

FIG. 2. (Color online) (a) Simulated polarization-dependent $4p$ core-level photoemission spectra along the [001] direction of Yb^{3+} ions assuming the CEF-split Γ_6 and Γ_7 ground states in cubic symmetry. The geometry for the simulations is the same as that in Fig. 1(a). (b) Same as (a), but $5p$ core-level photoemission spectra. The Gaussian and Lorentzian broadenings have been set to the same as those for the $4d$ photoemission spectra in Fig. 1(b).

polarization-dependent angle-resolved core-level photoemission spectra. The polarization and angular dependence of the multiplet-split peak structure reflects the outer localized anisotropic charge distributions determined by CEF, which is not restricted for the so far reported Yb^{3+} $3d$ photoemission spectra.

We have simulated the polarization-dependent angle-resolved core-level photoemission spectra due to the $l_c \rightarrow l_c + 1$ transitions on the basis of Eq. 8 for Yb^{3+} ions in cubic symmetry using the XTLS 9.0 program[33]. In Stevens formalism[34], the eightfold degenerate Yb^{3+} $J = 7/2$ state with one $4f$ hole splits by CEF in cubic symmetry into two doublets (Γ_6 and Γ_7) and one quartet (Γ_8), where the Γ_6, Γ_7, and Γ_8 $4f$ charge distributions are elongated along the [100], [111], and [110] directions, respectively[16,21]. In the simulations of the $4d$ and n_cp ($n_c = 4, 5$) core-level photoemission spectra, the full multiplet theory and the local CEF splitting are included. All atomic parameters such as the Coulomb and exchange interactions (Slater integrals) and the spin-orbit couplings have been obtained by Cowan's code[35] based on the Hartree-Fock method. The Slater integrals (spin-orbit couplings) are reduced to 88% (98% for the inner-core orbitals and 100% for the $4f$ orbital).

Simulated polarization-dependent $4d$ core-level photoemission spectra of Yb^{3+} ions with the Γ_6, Γ_7, and Γ_8 ground states along the [001] direction at the geometry shown in Fig. 1(a) are demonstrated in Fig. 1(b). As theoretically seen in the $3d_{5/2}$ core-level photoemission spectra[21], LDs defined by the difference in the spectral weight between the s- and p-polarization configurations as a function of binding energy are also clearly shown in the $4d$ photoemission spectra. For the Γ_6 and Γ_7 ground states, prominent LD is predicted around the relative binding energies of -8.5 and 0.4 eV. Even for the Γ_8 ground state, finite LD is predicted while the LD is markedly reduced compared with that for the Γ_6 and Γ_7 ground states. The reduction of LD for the Γ_8 ground state is ascribed to the fact that the $4f$ hole spatial distribution is the nearest to a spherical shape among these three states[21]. The simulations suggest that the finite angular dependence of the multiplet-split peak structure can be observed for single crystals even if we measure the spectra using a photoelectron spectrometer with an acceptance angle of ±several degrees at an unpolarized light excitation with no electric field along the propagation direction of the excitation lights.

Figure 2 shows the simulated angle-resolved $4p$ and $5p$ core-level photoemission spectra for the Γ_6 and Γ_7 ground

states, verifying complete absence of LD. These results are in a strong contrast to those in the $4d$ core-level spectra. LD is also absent for the Γ_8 state since the isotropic spectra are formed by the sum of spectra for the Γ_6, Γ_7, and Γ_8 states weighted by their degeneracy. Our simulation results indicate that the core-level excitation with $l_c \geq 2$ irrespective of n_c is essential for observing LD in the angle-resolved photoemission spectra of the systems in cubic symmetry. The LD in the core-level photoemission spectra can also be regarded as the consequence of the CEF splitting of the core levels due to the anisotropic outer charge distributions. It is well known that the degenerated n_cp core levels are not split by CEF in cubic symmetry with the fourth-order potential. Therefore, the p_x, p_y, and p_z orbitals are mutually equivalent in cubic symmetry, which leads to the complete absence of LD in the n_cp core-level spectra as shown in Fig. 2. The LD in the n_cp core-level photoemission spectra due to the anisotropic outer charge distribution would be observed for strongly correlated electron systems with lower symmetry than the cubic one.

In summary, we have shown the formulations and simulations of the linear polarization-dependent angle-resolved core-level photoemission for the ions under CEF. The finite LD and angular dependence of the multiplet-split core-level spectral shape reflecting the anisotropic outer localized charge distributions determined by the occupied orbital symmetry are expected at the d core-level excitations even for the systems in cubic symmetry.

We thank Y. Saitoh, H. Fujiwara, and T. Mori for fruitful discussions. This work was supported by JSPS and MEXT, Japan with the KAKENHI Grant Numbers JP16H04014 and JP16H01074. Y. Kanai was supported by the JSPS Research Fellowships for Young Scientists.

[1] M. Abbate, M. Sacchi, J. J. Wnuk, L. W. M. Schreurs, Y. S. Wang, R. Lof, and J. C. Fuggle, Phys. Rev. B **42**, 7914 (1990).
[2] S. Suzuki, T. Takahashi, T. Kusunoki, T. Morikawa, S. Sato, H. Katayama-Yoshida, A. Yamanaka, F. Minami, and S. Takekawa, Phys. Rev. B **44**, 5381 (1991).
[3] C. T. Chen, L. H. Tjeng, J. Kwo, H. L. Kao, P. Rudolf, F. Sette, and R. M. Fleming, Phys. Rev. Lett. **68**, 2543 (1992).
[4] F. Steglich, J. Aarts, C. D. Bredl, W. Lieke, D. Meschede, W. Franz, and H. Schäfer, Phys. Rev. Lett. **43**, 1892 (1979).
[5] N. D. Mathur, F. M. Grosche, S. R. Julian, I. R. Walker, D. M. Freye, R. K. W. Hselwimmer, and G. G. Lonzarih, Nature (London) **394**, 39 (1998).
[6] R. Settai, T. Takeuchi, and Y. Ōnuki, J. Phys. Soc. Jpn. **76**, 051003 (2007) and references therein.
[7] S. Nakatsuji, K. Kuga, Y. Machida, T. Tayama, T. Sakakibara, Y. Karaki, H. Ishimoto, S. Yonezawa, Y. Maeno, E. Pearson, G. G. Lonzarich, L. Balicas, H. Lee, and Z. Fisk, Nat. Phys. **4**, 603 (2008).
[8] K. Hanzawa and T. Kasuya, J. Phys. Soc. Jpn. **53**, 1809 (1984).
[9] A. Yatskar, W. P. Beyermann, R. Movshovich, and P. C. Canfield, Phys. Rev. Lett. **77**, 3637 (1996).
[10] D. Aoki, Y. Katayama, R. Settai, Y. Inada, Y. Ōnuki, H. Harima, and Z. Kletowski, J. Phys. Soc. Jpn. **66**, 3988 (1997).
[11] T. Onimaru and H. Kusunose, J. Phys. Soc. Jpn. **85**, 082002 (2016), and references therein.
[12] E. Zirngiebl, B. Hillebrands, S. Blumenröder, G. Güntherodt, M. Loewenhaupt, J. M. Carpenter, K. Winzer, and Z. Fisk, Phys. Rev. B **30**, 4052 (1984).
[13] T. Willers, B. Fåk, N. Hollmann, P. O. Körner, Z. Hu, A. Tanaka, D. Schmitz, M. Enderle, G. Lapertot, L. H. Tjeng, and A. Severing, Phys. Rev. B **80**, 115106 (2009).
[14] P. Hansmann, A. Severing, Z. Hu, M. W. Haverkort, C. F. Chang, S. Klein, A. Tanaka, H. H. Hsieh, H.-J. Lin, C. T. Chen, B. Fåk, P. Lejay, and L. H. Tjeng, Phys. Rev. Lett. **100**, 066405 (2008).
[15] T. Willers, Z. Hu, N. Hollmann, P. O. Körner, J. Gegner, T. Burnus, H. Fujiwara, A. Tanaka, D. Schmitz, H. H. Hsieh, H.-J. Lin, C. T. Chen, E. D. Bauer, J. L. Sarrao, E. Goremychkin, M. Koza, L. H. Tjeng, and A. Severing, Phys. Rev. B **81**, 195114 (2010).
[16] T. Willers, J. C. Cezar, N. B. Brookes, Z. Hu, F. Strigari, P. Körner, N. Hollmann, D. Schmitz, A. Bianchi, Z. Fisk, A. Tanaka, L. H. Tjeng, and A. Severing, Phys. Rev. Lett. **107**, 236402 (2011).
[17] T. Willers, D. T. Adroja, B. D. Rainford, Z. Hu, N. Hollmann, P. O. Körner, Y.-Y. Chin, D. Schmitz, H. H. Hsieh, H.-J. Lin, C. T. Chen, E. D. Bauer, J. L. Sarrao, K. J. McClellan, D. Byler, C. Geibel, F. Steglich, H. Aoki, P. Lejay, A. Tanaka, L. H. Tjeng, and A. Severing, Phys. Rev. B **85**, 035117 (2012).
[18] F. Strigari, T. Willers, Y. Muro, K. Yutani, T. Takabatake, Z. Hu, Y.-Y. Chin, S. Agrestini, H.-J. Lin, C. T. Chen, A. Tanaka, M. W. Haverkort, L. H. Tjeng, and A. Severing, Phys. Rev. B **86**, 081105(R) (2012).
[19] T. Willers, F. Strigari, N. Hiraoka, Y. Q. Cai, M. W. Haverkort, K.-D. Tsuei, Y. F. Liao, S. Seiro, C. Geibel, F. Steglich, L. H. Tjeng, and A. Severing, Phys. Rev. Lett. **109**, 046401 (2012).
[20] T. Mori, S. Kitayama, Y. Kanai, S. Naimen, H. Fujiwara, A. Higashiya, K. Tamasaku, A. Tanaka, K. Terashima, S. Imada, A. Yasui, Y. Saitoh, K. Yamagami, K. Yano, T. Matsumoto, T. Kiss, M. Yabashi, T. Ishikawa, S. Suga, Y. Ōnuki, T. Ebihara, and A. Sekiyama, J. Phys. Soc. Jpn. **83**, 123702 (2014).
[21] Y. Kanai, T. Mori, S. Naimen, K. Yamagami, H. Fujiwara, A. Higashiya, T. Kadono, S. Imada, T. Kiss, A. Tanaka, K. Tamasaku, M. Yabashi, T. Ishikawa, F. Iga, and A. Sekiyama, J. Phys. Soc. Jpn. **84**, 073705 (2015).
[22] J. W. Gadzuk, Phys. Rev. B **12**, 5608 (1975).
[23] S. M. Goldberg, C. S. Fadley, and S. Kono, J. Electron Spectrosc. Relat. Phenom. **21**, 285 (1980).
[24] H. Daimon, S. Imada, H. Nishimoto, and S. Suga, J. Electron Spectrosc. Relat. Phenom. **76**, 487 (1995).
[25] H. Nishimoto, T. Nakatani, T. Matsushita, S. Imada, H. Daimon, and S. Suga, J. Phys.: Condens. Matter **8**, 2715 (1996).
[26] J. H. Scofield, J. Electron Spectrosc. Relat. Phenom. **8**,

129 (1976).
[27] J. J. Yeh and I. Lindau, At. Data Nucl. Data Tables **32**, 1 (1985).
[28] M. B. Trzhaskovskaya, V. I. Nefedov, and V. G. Yarzhemsky, At. Data Nucl. Data Tables **77**, 97 (2001).
[29] M. B. Trzhaskovskaya, V. I. Nefedov, and V. G. Yarzhemsky, At. Data Nucl. Data Tables **82**, 257 (2002).
[30] M. B. Trzhaskovskaya, V. K. Nikulin, V. I. Nefedov, and V. G. Yarzhemsky, At. Data Nucl. Data Tables **92**, 245 (2006).
[31] O. Gunnarsson and K. Schönhammer, Phys. Rev. B **28**, 4315 (1983); **31**, 4815 (1985).
[32] T. Jo and A. Kotani, J. Phys. Soc. Jpn. **55**, 2457 (1986).
[33] A. Tanaka and T. Jo, J. Phys. Soc. Jpn. **63**, 2788 (1994).
[34] K.W. H. Stevens, Proc. Phys. Soc. London Sect. A **65**, 209 (1952).
[35] R. D. Cowan, *The Theory of Atomic Structure and Spectra* (University of California Press, Berkeley, 1981).